

Senescent RAW264.7 cells exhibit increased production of nitric oxide and release inducible nitric oxide synthase in exosomes

HIROKAZU HATTORI*, KAZUKI TAKAOKA*, MIHO UETA, MASAYUKI OSHITANI,
JOJI TAMAOKA, KAZUMA NOGUCHI and HIROMITSU KISHIMOTO

Department of Oral and Maxillofacial Surgery, Hyogo College of Medicine, Nishinomiya, Hyogo 663-8501, Japan

Received November 23, 2020; Accepted June 8, 2021

DOI: 10.3892/mmr.2021.12320

Abstract. Aging cells not only cease growing, but also secrete various proteins such as inflammatory cytokines. This secretory phenomenon is known as the senescence-associated secretory phenotype (SASP). The aim of the present study was to elucidate the effects of senescence on the differentiation of osteoclast precursors (OCPs) and corresponding SASP. RAW264.7 cells were used as OCPs and were cultured to passage (P)5, P10 and P20. Cell proliferation assays, senescence-associated β -galactosidase staining and telomere length quantification were subsequently performed, and it was revealed that replicative senescence was induced at P20. In addition, the level of tartrate-resistant acid phosphatase activity in P20 cells treated with receptor activator of nuclear factor- κ B ligand was significantly lower than that in P5 and P10 cells. The SASP factors interleukin-6, tumour necrosis factor- α and nitric oxide were significantly increased in P20 culture supernatants compared with those in P5 and P10 supernatants. Furthermore, the number of exosomes at P20 was increased compared with that at P5 and P10, and inducible nitric oxide synthase (iNOS) was expressed in exosomes at P20, but not in exosomes at P5. In conclusion, the present study revealed that senescent RAW264.7 cells exhibit increased expression of SASP factors and release iNOS in exosomes.

Introduction

Senescence is defined as the decline of physiological functions with aging and affects most living organisms (1).

Correspondence to: Dr Kazuki Takaoka, Department of Oral and Maxillofacial Surgery, Hyogo College of Medicine, 1-1 Mukogawa-cho, Nishinomiya, Hyogo 663-8501, Japan
E-mail: ktaka@hyo-med.ac.jp

*Contributed equally

Key words: cellular senescence, senescence-associated secretory phenotype, osteoclast precursors, RAW264.7 cells, bone microenvironment

Adverse changes at cellular and molecular levels caused by senescence lead to increased risks of several diseases, such as cancer, cardiovascular diseases, diabetes, osteopenia and osteoporosis (2).

Bone is constantly remodelled throughout life by the balanced activity of osteoblastic bone formation and osteoclastic bone resorption; however, the balance between bone resorption and formation is lost due to aging, which results in age-related bone loss, including osteoporosis, and an increased risk of fracture (3). Some aging mechanisms are related to changes in the expression and signalling of local factors in the bone microenvironment (4). There are three important cell types for bone remodelling: Osteoblasts, osteocytes and osteoclasts (OCs) (5). Osteocyte and osteoblast senescence in the bone microenvironment has been investigated (6), whereas OC and OC precursor (OCP) senescence in the bone microenvironment has not been analysed in detail. OCs differentiate from OCPs, which are precursor cells derived from the monocyte/macrophage lineage (7). OCPs are recruited from the bloodstream into bone by various factors released at sites undergoing resorption in the bone microenvironment, and OCPs are subsequently differentiated into OCs responsible for bone resorption (7). Cao *et al* (8) revealed that aging is accompanied by increased receptor activator of nuclear factor (NF)- κ B ligand (RANKL) and macrophage colony-stimulating factor expression, which can increase stromal/osteoblastic cell-induced osteoclastogenesis and expansion of the OCP pool. If the number of OCPs that cannot differentiate increases, the number of aging OCPs increases. Along with stem cell aging, their ability to differentiate into various cell types is also altered (9).

Senescence is an unexplained phenomenon, which occurs in the microenvironment where bone remodelling occurs. In recent years, it has become clear that senescent cells do not simply cease growing but also secrete various proteins, such as inflammatory cytokines and chemokines (10). This secretory phenomenon is known as the senescence-associated secretory phenotype (SASP). SASP is predominantly exhibited by senescent osteoprogenitors, myeloid cells and osteocytes (11,12). Farr *et al* (12) suggested that senescent osteocytes and their SASP contribute to age-related bone loss by assessing the critical roles of osteocytes in orchestrating bone remodelling. However, additional senescent cell types in the bone microenvironment and their corresponding SASP may be uncovered.

The aim of the present study was to elucidate senescent OCPs and their corresponding SASP.

Materials and methods

Cell culture. RAW264.7 cells for use as OCPs were obtained from the RIKEN BioResource Center. Cells were cultured in α -minimum essential medium (α -MEM; Gibco; Thermo Fisher Scientific, Inc.) supplemented with 10% foetal bovine serum (FBS; Gibco; Thermo Fisher Scientific, Inc.), 100 U/ml penicillin and 100 μ g/ml streptomycin at 37°C in a humidified atmosphere containing 5% CO₂ and were passaged every 3–4 days. RAW264.7 cell-derived OCs appear to form better in response to RANKL stimulation after passage (P)4, but cannot form after P18–20 (13). Therefore, it was assumed that cells at P20 would be replicative senescent cells, and RAW264.7 cells were grown until P5, P10 and P20.

Cell proliferation assay. RAW264.7 cells (P5, P10, and P20) were seeded on 96-well culture plates at 5x10³ cells/well and were cultured for 1–4 days. Subsequently, the WST-8 reagent in a Cell Counting Kit-8 (Dojindo Molecular Technologies, Inc.) was added to the cells (10 μ l/well), followed by incubation for 2 h at 37°C. The cell proliferation was determined by measuring the absorbance at 450 nm using a microplate reader (Benchmark Plus™ Microplate Spectrophotometer; Bio-Rad Laboratories, Inc.) (14).

Senescence-associated β -galactosidase (SA- β -gal) staining and flow cytometric analysis. SA- β -gal staining was performed using a Cellular Senescence Detection Kit-SPiDER- β gal (Dojindo Molecular Technologies, Inc.) in accordance with the manufacturer's instructions. RAW264.7 cells (P5, P10 and P20) were seeded in a 35-mm culture dish at a density of 5x10⁴ cells/dish and incubated overnight. The cells were washed with 2 ml Hank's balanced salt solution (HBSS) and bafilomycin A1 working solution (1 ml) was added to the culture dish for 1 h. SPiDER- β gal working solution (1 ml) and 1 mg/ml Hoechst 33342 (1 μ l; Dojindo Molecular Technologies, Inc.) were then added to the culture and the cells were incubated for 30 min. After the supernatant was removed, the cells were washed twice with HBSS (2 ml) and HBSS (2 ml) was added to the culture dish. All images were obtained under a fluorescence microscope (Ti-E; Nikon Corporation). The percentage of positive cells was manually computed in five random fields per section at x400 magnification (15).

Flow cytometry was performed using a protocol similar to SA- β -gal staining. RAW264.7 cells (P5, P10, and P20) were seeded in a 35-mm culture dish at a density of 1x10⁵ cells/dish. Cells were treated in the same manner as for SA- β -gal staining; however, they were not treated with Hoechst 33342. Flow cytometric analysis was performed using a BD FACSCalibur and BD FACSDiva (v8.0.1; BD Biosciences).

Quantification of telomere length. Genomic DNA was isolated from RAW264.7 cells (P5, P10, and P20) by the phenol-chloroform extraction method using phenol/chloroform/isoamyl alcohol (25:24:1; cat. no. 311-90151, Nippon Gene Co., Ltd.). Total telomere length was determined by a

telomere hybridization protection assay using 0.2 μ g denatured genomic DNA as described previously (16).

Tartrate-resistant acid phosphatase (TRAP) staining. RAW264.7 cells (P5, P10, and P20) were seeded on 12-well culture plates at 2.5x10³ cells/well. The cells were treated with RANKL (50 ng/ml; Oriental Yeast Co. Ltd.) for 7 days at 37°C. The culture medium supplemented with RANKL was replaced every 3 days. Subsequently, the cells were stained using a TRAP staining kit (Cosmo Bio Co., Ltd.) in accordance with the manufacturer's instructions. TRAP-positive multinucleated cells were identified as OCs under the light microscope (Ti-E; Nikon Corporation) (14).

TRAP activity assay. RAW264.7 cells (P5, P10, and P20) were seeded on 96-well culture plates at 2x10³ cells/well. The cells were treated with RANKL (50 ng/ml) for 4 days at 37°C. The cells were then fixed with ethanol/acetone as described previously (17) and evaluated for TRAP activity using a TRAP solution kit (Oriental Yeast Co. Ltd.) in accordance with the manufacturer's instructions. Briefly, 150 μ l 50 mM citrate buffer (pH 4.5) containing 5.5 mM p-nitrophenol phosphate and 10 mM sodium tartrate was added to each well. After incubation for 60 min at room temperature, 50 μ l 0.1 N NaOH was added and the absorbance at 405 nm was determined using a microplate reader (14).

Measurement of interleukin (IL)-6, tumour necrosis factor (TNF)- α and nitric oxide (NO) production. RAW264.7 cells (P5, P10 and P20) at 1x10⁶ cells/well in 24-well culture plates were cultured for 24 h in serum-free medium. The culture supernatants were centrifuged at 4°C for 10 min at 1,000 x g, harvested and used immediately. IL-6 was measured via a quantitative sandwich enzyme immunoassay method using a Mouse IL-6 Assay Kit (cat. no. 27768; Immuno-Biological Laboratories Co., Ltd.) in accordance with the manufacturer's instructions. Optical density (OD) values at 450 nm were measured using a microplate reader. The levels of TNF- α in culture supernatants were measured using a TNF- α Mouse ELISA kit Quantikine (cat. no. MTA00B; R&D Systems, Inc.) in accordance with manufacturer's instructions. OD values at 450 nm were measured using a microplate reader. The levels of NO₂⁻/NO₃⁻ in culture supernatants were measured using an NO₂⁻/NO₃⁻ Assay Kit-C II consisting of Griess reagents (cat. no. NK05; Dojindo Molecular Technologies, Inc.) according to the manufacturer's instructions. Samples were reacted with Griess reagent and absorbance was measured at 540 nm using a microplate reader. It is common practice to quantitate total NO₂⁻/NO₃⁻ as a measure of NO levels (18).

Isolation and quantification of exosomes. Exosome isolation using an ExoQuick exosome precipitation kit (System Biosciences) was performed in accordance with the manufacturer's instructions. Briefly, 1x10⁶ RAW264.7 cells (P5, P10 and P20) were cultured for 48 h in α -MEM containing 10% exosome-depleted FBS (System Biosciences). The culture supernatant was collected and centrifuged at 3,000 x g for 15 min at 4°C to remove intact cells and cell debris. ExoQuick exosome precipitation solution (2 ml) was added to 10-ml culture supernatant. The resulting solution was

mixed by inverting the tube and then incubated for 12 h at 4°C. This mixture was then centrifuged at 1,500 x g for 30 min at room temperature. The supernatant was discarded and the precipitate consisted of exosomes (19). Exosome quantification and western blot analysis of exosomes were performed using the exosome pellets. For exosome quantification, the exosome pellets were resuspended in Exosome Binding Buffer (a component of the CD63 ExoELISA kit). The total number of exosomes was determined using a CD63 ExoELISA kit (cat. no. EXOEL-CD63A-1, System Bioscience) following the manufacturers' instructions; this kit detects the general exosome marker CD63 by ELISA (20). For western blot analysis of exosomes, the exosome pellets were resuspended in radioimmunoprecipitation buffer (RIPA; cat. no. sc-24948; Santa Cruz Biotechnology, Inc.). Western blot analysis of exosomes was performed using the resulting solution. Exosomes prepared from RAW264.7 cells at P5, P10 and P20 were termed Exo-P5, Exo-P10 and Exo-P20, respectively.

Nanosight particle tracking analysis. The isolated exosome pellets were diluted at 1:5,000 with PBS and injected into the Nanosight LM10 system (Malvern Panalytical Ltd.). Capture and analysis settings were manually set in accordance with the manufacturer's instructions. Particles were visualised by laser light scattering and their Brownian motion was captured on digital video. Five separate runs were conducted for each sample. The recorded videos were analysed using Nanoparticle Tracking Analysis 2.3 software (Malvern Panalytical Ltd.) and the size distribution of particles was determined (21).

Western blot analysis. RAW264.7 cells (P5, P10 and P20) were seeded in 60-mm culture plates and lysed using RIPA buffer (cat. no. sc-24948; Santa Cruz Biotechnology, Inc.). The lysates and exosomal proteins were analysed by western blotting as described previously (22). The following primary antibodies were used: Rabbit polyclonal antibodies against p53 (1:200; cat. no. sc-6243; Santa Cruz Biotechnology, Inc.), transforming growth factor β 1 (TGF- β 1; 1:1,000; cat. no. 3711; Cell Signaling Technology, Inc.), histone H2A.X (H2A.X; 1:1,000; cat. no. 2595; Cell Signaling Technology, Inc.), inducible nitric oxide synthase (iNOS; 1:2,000; cat. no. ab3523; Abcam), NF- κ B (1:1,000; cat. no. GTX102090; GeneTex, Inc.), CD63 (1:1,000; cat. no. EXOAB-CD63A-1; System Biosciences) and mammalian target of rapamycin (mTOR; 1:1,000; cat. no. 2972; Cell Signaling Technology, Inc.), rabbit monoclonal antibodies against tumour susceptibility gene 101 (TSG101; 1:1,000; cat. no. ab125011; Abcam) and phosphorylated (p)-H2A.X (Ser139) (1:1,000; cat. no. 2577; Cell Signaling Technology, Inc.), mouse monoclonal antibodies against receptor activator of NF- κ B (RANK; 1:500; cat. no. ab13918; Abcam), hypoxia-inducible factor (HIF)-1 α (1:1,000; cat. no. NB100-131; Novus Biologicals LLC) and nuclear factor of activated T cells cytoplasmic 1 (NFATc1; 1:200; cat. no. sc-7294; Santa Cruz Biotechnology, Inc.), and a goat polyclonal antibody against β -actin (1:1,000; cat. no. sc-1616; Santa Cruz Biotechnology, Inc.). The secondary antibodies used were HRP-conjugated anti-goat IgG (1:2,000; cat. no. P0449; Dako; Agilent Technologies, Inc.), HRP-conjugated anti-mouse IgG (1:1,000; cat. no. 7076; Cell Signaling Technology, Inc.) and HRP-conjugated

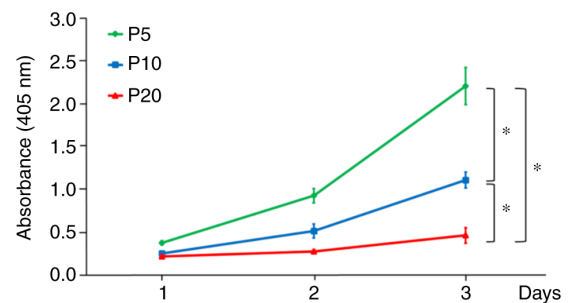


Figure 1. Cell proliferation assay. RAW264.7 cells at 5×10^3 cells/well were cultured for 1, 2 or 3 days and then proliferation was assessed using the WST-8 reagent in the Cell Counting Kit-8. * $P < 0.05$ (one-way ANOVA and Tukey-Kramer test). P, passage.

anti-rabbit IgG (1:10,000; cat. no. 458; MBL International Co.). Signals were detected by chemiluminescence using a Pierce SuperSignal Western Blotting Kit (Pierce; Thermo Fisher Scientific, Inc.). β -actin was evaluated as an internal control to confirm equal amounts of total protein.

Statistical analysis. All data are expressed as the mean \pm standard deviation of three independent experiments. Statistical analyses were performed using one-way ANOVA and Tukey-Kramer test for intergroup comparisons in each experiment. $P < 0.05$ was considered to indicate a statistically significant difference.

Results

Serial passaging leads to replicative senescence. A decrease in cell proliferation was detected during the progression of replicative senescence. The proliferation of cells at P20 was significantly lower than that of cells at P5 and P10 (Fig. 1). In addition, the protein expression levels of mTOR in cells at P20 were decreased compared with those at P5 and P10 (Fig. 2A). The protein expression levels of p-H2A.X in cells at P20 were increased compared with those at P5 and P10 (Fig. 2A). Telomere length at P20 was decreased compared with that at P5 and P10 (Fig. 2B). The protein expression levels of p53 in cells at P10 was increased compared with those at P5; however, when cells reached P20 and exhibited reduced proliferation, the protein expression levels of p53 were lower than those at P10 (Fig. 2A).

RAW264.7 cells at P5, P10 and P20 were subjected to SA- β -gal staining (Fig. 2C). The senescent status of the cell cultures was measured by SA- β -gal quantitation. SA- β -gal-positive cells at P20 were significantly increased (63.2%) compared with those at P5 (4.5%) and P10 (23.2%) (Fig. 2D). Furthermore, using flow cytometry, the fluorescence intensity of SA- β -gal staining was analysed (Fig. 2E). The fluorescence intensity of cells at P20 was increased compared with that at P5 and P10. Thus, it was confirmed that cells at P20 were replicative senescent cells.

Differentiation of RAW264.7 cells. To investigate the effect of replicative senescence on OC differentiation, TRAP staining was performed to determine TRAP enzymatic activity. The level of TRAP enzymatic activity in cultured

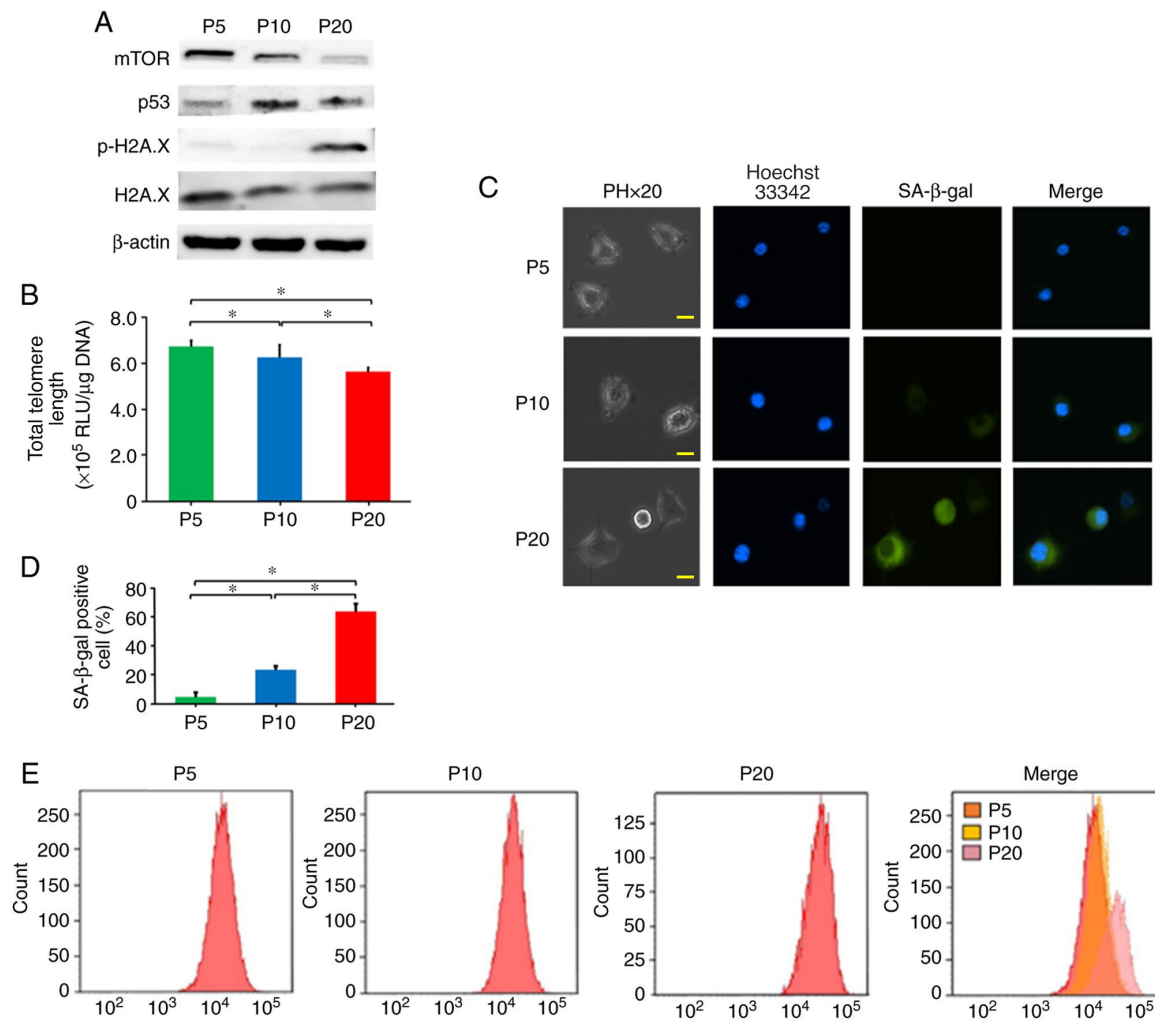


Figure 2. Induction of replicative senescence by serial passaging of RAW264.7 cells. (A) Measurement of protein expression levels of mTOR, p-H2A.X, H2A.X and p53 by western blot analysis. (B) Telomere length. (C) SA-β-gal staining. SA-β-gal was labelled with green fluorescence and nuclei were stained with Hoechst 33342. Scale bars=10 μ m. (D) Percentage of cells positive for SA-β-gal staining. * P <0.05 (one-way ANOVA and Tukey-Kramer test). (E) Flow cytometric analysis of replicative senescence, as determined by SA-β-gal staining. H2A.X, histone H2A.X; mTOR, mammalian target of rapamycin; p-, phosphorylated; RLU, relative light units; SA-β-gal, senescence-associated β-galactosidase.

cell lysates has been reported to be correlated with the relative number of OCs observed by TRAP staining (23). On day 7, RANKL induced the formation of large multinucleated (≥ 5 nuclei) OC-like cells at P5 and P10; however, there were no TRAP-positive multinucleated cells detected at P20 (Fig. 3A). To confirm the potential effect of replicative senescence on RANKL-induced OC differentiation, TRAP enzymatic activity was determined. The level of TRAP activity in cells treated with RANKL at P20 was significantly lower than that at P5 and P10 (Fig. 3B). Furthermore, the protein expression levels of RANK and NFATc1 were increased in cells treated with RANKL (50 ng/ml) at P5 and P10 compared with those at P20 (Fig. 3C). These results suggested that RAW264.7 cells cannot differentiate into OC-like cells while aging.

Effect of senescence in RAW264.7 cells on SASP factors. The expression levels of SASP factors TGF-β1, iNOS and NF-κB in cells at P20 were increased compared with those at P5 and P10. In addition, HIF-1α protein expression was increased in cells at P20 compared with that at P5 and P10 (Fig. 4A). Furthermore, the present study detected secretion of SASP

factors IL-6, TNF-α and NO from RAW264.7 cells. The levels of IL-6, TNF-α and NO in the culture supernatants at P20 were significantly increased compared with those at P5 and P10 (Fig. 4B).

Effect of senescence in RAW264.7 cells on isolation of exosomes. To characterise vesicles released from RAW264.7 cells, size detection was performed by Nanosight particle tracking analysis (Fig. 5A). Vesicle size peaks at P5, P10 and P20 were 128, 100 and 133 nm, respectively. Exosomes are vesicles derived from the endosomal membrane with diameters 40–150 nm (24,25). Subsequently, the expression of exosome markers (CD63 and TSG101) were detected by western blotting to confirm the identity of exosomes (Fig. 5B). The results indicated successful isolation of exosomes from RAW264.7 cells. Expression of tetraspanin protein CD63 was detected by ELISA to determine the concentration of exosomes (Fig. 5C). The number of exosomes at P20 was increased compared with that at P5 and P10. In addition, iNOS was detected in exosomes at P10 and P20, but not at P5; however, TGF-β1 and HIF-1α were not detected in exosomes at P5, P10 and P20 (Fig. 5B). In

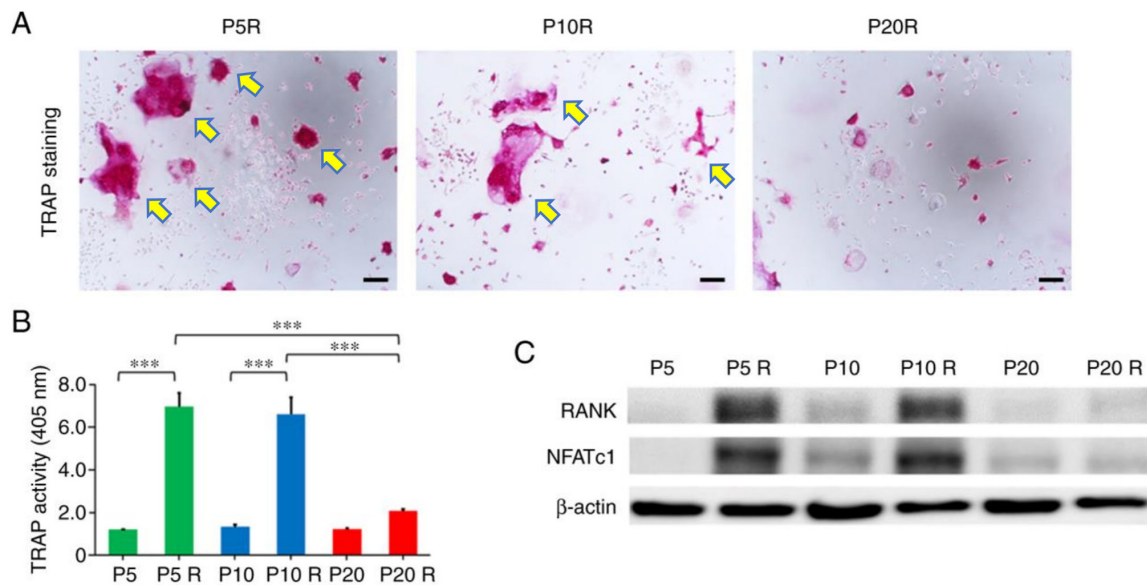


Figure 3. Effect of senescence on RAW264.7 cell differentiation. (A) TRAP staining. Arrows indicated large multinucleated (≥ 5 nuclei) OC-like cells. Scale bars, 100 μm . (B) TRAP activity. *** $P < 0.001$ (one-way ANOVA and Tukey-Kramer test). (C) Measurement of protein expression levels of RANK and NFATc1 by western blot analysis. NFATc1, nuclear factor of activated T cells cytoplasmic 1; P, passage; P5 R, P5 + RANKL; P10 R, P10 + RANKL; P20 R, P20 + RANKL; RANK, receptor activator of NF- κ B; RANKL, RANK ligand; TRAP, tartrate-resistant acid phosphatase.

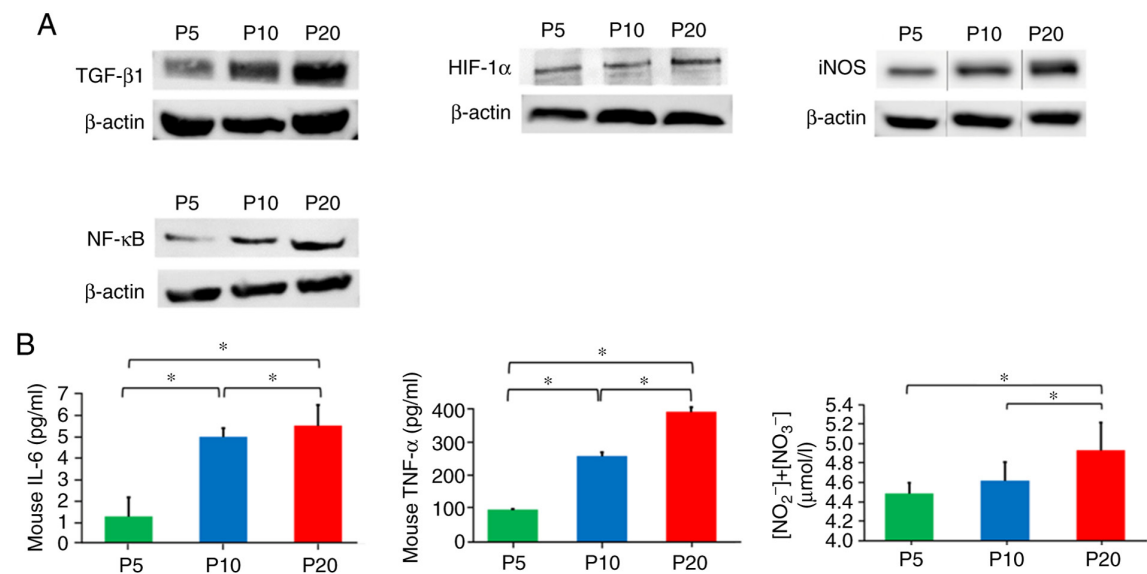


Figure 4. Effect of senescence on senescence-associated secretory phenotype factors in RAW264.7 cells. (A) Measurement of protein expression levels of TGF- β 1, HIF-1 α , iNOS and NF- κ B, as determined by western blot analysis. (B) ELISA was used to determine NO₂⁻/NO₃⁻, IL-6 and TNF- α levels in the culture medium. Data are presented as the mean \pm standard deviation. * $P < 0.05$ (one-way ANOVA and Tukey-Kramer test). HIF-1 α , hypoxia-inducible factor-1 α ; IL-6, interleukin 6; iNOS, inducible nitric oxide synthase; NF- κ B, nuclear factor- κ B; NO, nitric oxide; P, passage; TGF- β 1, transforming growth factor β 1; TNF- α , tumour necrosis factor- α .

these SASP factors, it was suggested that only iNOS may be contained in exosomes and specifically released.

Discussion

Cellular senescence was initially described as the finite proliferative capacity of cultured normal human fibroblasts by Hayflick and Moorhead in 1961 (26). After its discovery, cellular senescence was defined as a status characterised by irreversible arrest of cell proliferation (27). Growing evidence has suggested that replicative senescence can be used as

an *in vitro* surrogate for aging (6,28-30). The present study established replicative senescent cells by serial passaging of RAW264.7 cells. RAW264.7 cells are widely known as OCPs and serve an important role in *in vitro* studies (13,31,32). Cellular senescence is defined by irreversible arrest of the cell cycle, changes in cell morphology (large and flattened cells) and expression of specific biomarkers (33). Among the specific biomarkers of senescent cells, the lysosomal enzyme SA- β -gal is widely used (34,35). Induction of replicative senescence in RAW264.7 cells at P20 was confirmed by SA- β -gal staining. In addition, induction of p53 causes cellular senescence by

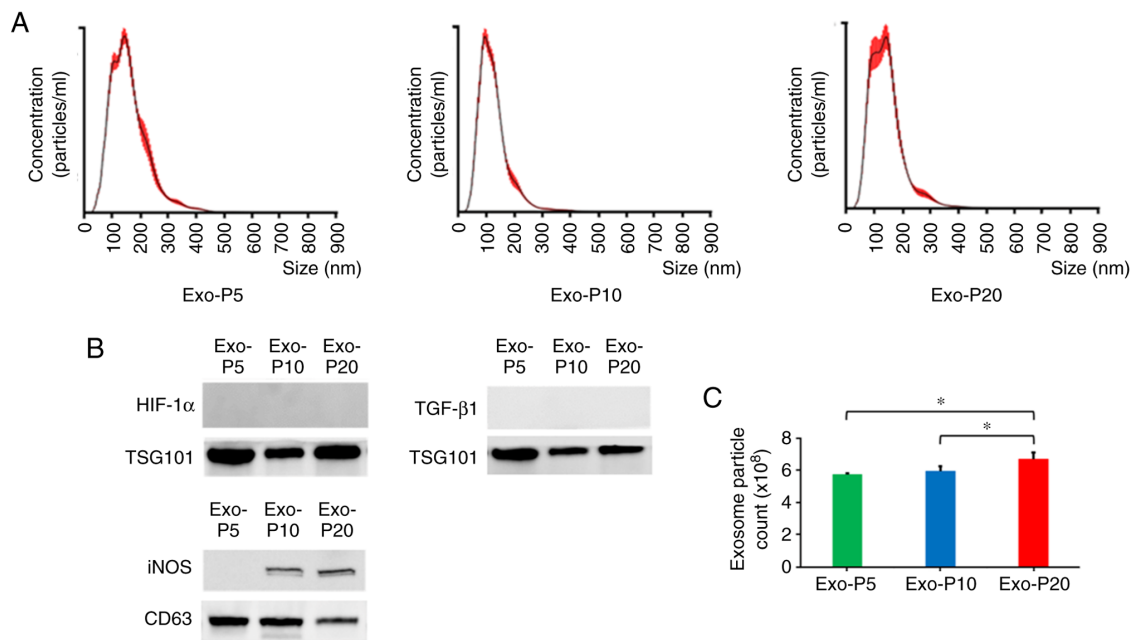


Figure 5. Characterisation of exosomes isolated from RAW264.7 cells. (A) Size distribution of exosomes was analysed by using a NanoSight LM10. Red error bars indicate ± 1 standard error of the mean. (B) Measurement of protein expression levels of exosome markers (CD63 and TSG101), TGF- β 1, HIF-1 α and iNOS by western blot analysis. (C) Exosome quantification. The total number of exosomes derived from RAW264.7 cells (P5, P10 and P20) was analysed by detecting the expression levels of the exosomal marker CD63. Data are presented as the mean \pm standard deviation. * $P < 0.05$ (one-way ANOVA and Tukey-Kramer test). HIF-1 α , hypoxia-inducible factor-1 α ; iNOS, inducible nitric oxide synthase; P, passage; TGF- β 1, transforming growth factor β 1; TSG101, tumour susceptibility gene 101.

reversible cell cycle arrest (36–38). It is known that p53 can inhibit the mTOR pathway (39,40); mTOR signalling regulates cell growth and metabolism (41). In the present study, the protein expression levels of p53 in cells at P10 were increased compared with those at P5; however, the protein expression levels of p53 in cells at P20 were comparatively lower than those at P10. p53 functions decline with senescence and SASP is more intense when cells lose the functions of p53 (10,42). The growth curve of replicative senescent cells at P20 was almost flat and mTOR protein expression in cells at P20 was decreased compared with that at P5. Conversely, the protein expression levels of p-H2A.X in cells at P20 were increased compared with those at P5. Telomere length at P20 was also decreased compared with that at P5. Therefore, the present study confirmed that cells at P20 were replicative senescent cells.

The present study observed differences in the ability of RAW264.7 cells to differentiate into OCs, which depended on passage number. A previous study reported that RAW264.7 cells do not differentiate into OCs in response to RANKL stimulation at P18–20 (13). The present results demonstrated that the level of TRAP activity in cells treated with RANKL at P20 was significantly lower than that at P5 and P10. Moreover, cellular senescence reduced RANKL-induced osteoclastic differentiation of RAW264.7 cells by inhibiting RANK expression. Cellular senescence also attenuated RANKL-induced TRAP activity and the protein expression levels of NFATc1. These results suggested that OCPs may gradually lose their self-renewal and regenerative potentials, and cannot differentiate into OCs while aging. As a result, the number of senescent OCPs in the bone microenvironment may continue to increase because numerous OCPs are unable to differentiate into OCs.

SASP is a phenomenon in which senescent cells secrete proinflammatory cytokines, chemokines, growth factors and proteases (43). A beneficial function of SASP may be promotion of immune cell migration through secretion of proinflammatory cytokines (44). SASP is characterised by high level secretion of the cytokine IL-6, which is a crucial mediator of inflammation (45). Circulation of proinflammatory cytokines, such as IL-6, can induce not only cancer, but also various chronic inflammatory diseases (46). There are >60 known SASP factors, including ILs, chemokines and inflammatory molecules, such as TGF- β 1, IL-6, TNF- α and NO (47). Accumulation of senescent cells can lead to tissue damage by increased signalling of proinflammatory cytokines caused by propagation of oxidative stress due to mitochondrial dysfunction in neighbouring cells (48). Farr *et al* (12,49) reported that multiple senescent cell types, such as osteoprogenitors, myeloid cells, B cells, T cells and osteocytes, accumulated in the bone microenvironment with aging *in vivo* and suggested that senescent osteocytes may be linked to aging-associated bone loss. The present study focused on OCPs as senescent cells that affect the bone microenvironment. The results of the present study detected increases in the protein expression levels of TGF- β 1, NF- κ B and iNOS in senescent RAW264.7 cells, and increases in SASP factors, such as IL-6, TNF- α and NO, in the culture supernatant of senescent RAW264.7 cells. These results suggested high amounts of SASP factors (e.g., IL-6, TNF- α and NO) in the bone microenvironment.

TNF- α is a proinflammatory cytokine and potent inducer of bone resorption, which serves major roles in bone metabolism and inflammatory bone diseases (50). TNF- α directly induces the formation of TRAP-positive multinucleated OCs from OCPs in the absence of RANKL-mediated activation

of NF- κ B signalling (51). In addition, TNF- α can induce RANK expression in OCPs (52). However, in the present study, RAW264.7 cells exhibited inhibition of osteoclastogenesis after senescence, which were unaffected by TNF- α . Although TNF- α expression was increased in P20 cells, it did not induce RANK expression and formation of TRAP-positive multinucleated cells.

IL-6 is believed to indirectly induce production of RANKL by osteoblastic/stromal cells, which in turn stimulates OC activity and the commitment of OCPs into mature OCs (53). In addition, IL-6 has a direct effect on OC activity via differential regulation of RANKL-induced OC formation by specifically modulating phosphorylation of NF- κ B, extracellular signal-regulated kinase and c-Jun N-terminal kinase in a RANKL concentration-dependent manner; a stimulatory effect is observed under the condition of low RANKL, whereas an inhibitory effect is observed when the level of RANKL is markedly enhanced (54). Yokota *et al* (55) reported that the combination of TNF- α and IL-6 differentiated TRAP-positive multinucleated cells that resemble OCs, which had *in vitro* and *in vivo* bone resorption activities. Although TNF- α and IL-6 drive osteoclastogenesis, the present study revealed that RAW264.7 cells had inhibited osteoclastogenesis after senescence and that inhibition of osteoclastogenesis by NO exceeded acceleration of osteoclastogenesis by TNF- α and IL-6 in senescent OCPs.

OC formation and bone resorption are inhibited by elevated levels of the multifunctional signal molecule NO *in vivo* and *in vitro* (56-58). NO is a multifunctional gaseous molecule produced by NOS using L-arginine and molecular oxygen as substrates. It is known that NOS has three major isoforms: Neuronal NOS and endothelial NOS, which are constitutively expressed in cells, and iNOS, the expression of which is induced by inflammatory cytokines, endotoxins, hypoxia and oxidative stress (59,60). iNOS continuously produces a high concentration of NO (61). Zheng *et al* (62) reported that RANKL may induce iNOS expression in OCPs and revealed that high NO concentrations produced by iNOS inhibited OC differentiation. NO inhibited differentiation of OCPs after senescence in the bone microenvironment, which increased senescent OCPs. The present results demonstrated that the protein expression levels of HIF-1 α and iNOS at P20 were increased compared with those at P5 and P10. HIF-1 α induces NO production by induction of iNOS in mouse macrophages (63). HIF signalling is both necessary and sufficient to inhibit osteoclastogenesis through modulation of osteoprotegerin (64). From this viewpoint of SASP factors, the present results indicated that inhibition of osteoclastogenesis by NO exceeded acceleration of osteoclastogenesis by TNF- α and IL-6 in senescent OCPs.

Exosomes are vesicles derived from the endosomal membrane with diameters between 40 and 150 nm (24,25). Pools of exosomes are packed in multivesicular endosomes (MVEs) and released into the extracellular space after fusion of MVEs with the plasma membrane (24,65). Various proteins, lipids and nucleic acids in exosomes cause functional and physiological changes via transmission to other cells, and exosomes have important roles in intercellular communication (66,67). The results of the present study demonstrated that the number of exosomes at P20 was significantly higher than

that at P5 and P10. In addition to secretory proteins, senescent cells may exhibit increased secretion of exosomes (68). In the present study, SASP factors in exosomes were analysed by western blotting. The protein expression of iNOS was detected in exosomes at P20 and P10, but not at P5. Exosomes transmit carried signals to distant tissues and cells by circulating in body fluids, the contents of exosomes can reflect the physiological and pathological processes in cells (69). The present results suggested that iNOS-containing senescent OCP-derived exosomes may affect cellular communication not only locally in neighbouring cells, but also distally and systemically. iNOS-containing exosomes may be involved in inflammatory processes that serve pivotal roles in a large number of pathological states, including bone-destructive diseases, rheumatoid arthritis, inflammatory diseases and cancer.

In conclusion, cellular senescence reduced RANKL-induced osteoclastic differentiation of RAW264.7 cells by inhibiting RANK expression. In addition, senescent RAW264.7 cells exhibited increased production of SASP factors (IL-6, TNF- α and NO) and increased release of iNOS in exosomes. It is possible that clarification of the association between cellular senescence and SASP in OCPs may improve understanding of age-related bone changes and bone disorders, and further studies are required *in vivo*.

Acknowledgements

The authors would like to thank Ms. Shinobu Osawa M.Sc. (Department of Oral and Maxillofacial Surgery, Hyogo College of Medicine, Nishinomiya, Japan) for technical assistance.

Funding

The present study was supported by JSPS KAKENHI (grant nos. 18K09825 and 21K10106 to KT, 18K17124 to JT and 19K19182 to MU) and by a Grant-in-Aid for Graduate Students, Hyogo College of Medicine, 2020 (to HH).

Availability of data and materials

The datasets used and/or analysed during the study are available from the corresponding author on reasonable request.

Authors' contributions

HH, KT and KN conceived and designed the study. HH, KT, MU, MO and JT performed the experiments. HH, KT and MU analysed the data. HH, KT, MU and HK interpreted the data. HH, KT and HK wrote the manuscript. KT and HK confirm the authenticity of all the raw data. All authors read and approved the final manuscript.

Ethics approval and consent to participate

Not applicable.

Patient consent for publication

Not applicable.

Competing interests

The authors declare that they have no competing interests.

References

- López-Otín C, Blasco MA, Partridge L, Serrano M and Kroemer G: The hallmarks of aging. *Cell* 153: 1194-1217, 2013.
- Singh T and Newman AB: Inflammatory markers in population studies of aging. *Ageing Res Rev* 10: 319-329, 2011.
- Roberts S, Colombari P, Sowman A, Mennan C, Roling HD, Guicheux J and Edwards JR: Ageing in the musculoskeletal system: Cellular function and dysfunction throughout life. *Acta Orthop* 87: 15-25, 2016.
- Marie PJ: Bone cell senescence: Mechanisms and perspectives. *J Bone Miner Res* 29: 1311-1321, 2014.
- Katsimbri P: The biology of normal bone remodelling. *Eur J Cancer Care (Engl)*: 26: e12740, 2017.
- Han BI, Hwang SH and Lee MA: Progressive reduction in autophagic capacity contributes to induction of replicative senescence in Hs68 cells. *Int J Biochem Cell Biol* 92: 18-25, 2017.
- Boyce BF, Zuscik MJ and Xing L: Biology of bone and cartilage. In: *Genetics of Bone Biology and Skeletal Disease*. Thakker RV, Eisman J, Igarashi T and Whyte MP (eds). Elsevier, London, pp3-24, 2012.
- Cao JJ, Wronski TJ, Iwaniec U, Phleger L, Kurimoto P, Boudignon B and Halloran BP: Aging increases stromal/osteoblastic cell-induced osteoclastogenesis and alters the osteoclast precursor pool in the mouse. *J Bone Miner Res* 20: 1659-1668, 2005.
- Ahmed AS, Sheng MH, Wasnik S, Baylink DJ and Lau KW: Effect of aging on stem cells. *World J Exp Med* 7: 1-10, 2017.
- Coppe JP, Patil CK, Rodier F, Sun Y, Munoz DP, Goldstein J, Nelson PS, Desprez PY and Campisi J: Senescence-associated secretory phenotypes reveal cell-nonautonomous functions of oncogenic RAS and the p53 tumor suppressor. *PLoS Biol* 6: 2853-2868, 2008.
- Kim HN, Chang J, Shao L, Han L, Iyer S, Manolagas SC, O'Brien CA, Jilka RL, Zhou D and Almeida M: DNA damage and senescence in osteoprogenitors expressing *Osx1* may cause their decrease with age. *Aging Cell* 16: 693-703, 2017.
- Farr JN, Fraser DG, Wang H, Jaehn K, Ogronnik MB, Weivoda MM, Drake MT, Tchkonja T, LeBrasseur NK, Kirkland JL, *et al*: Identification of senescent cells in the bone microenvironment. *J Bone Miner Res* 31: 1920-1929, 2016.
- Collin-Osdoby P and Osdoby P: RANKL-mediated osteoclast formation from murine RAW264.7 cells. *Methods Mol Biol* 816: 187-202, 2012.
- Ueta M, Takaoka K, Yamamura M, Maeda H, Tamaoka J, Nakano Y, Nouchi K and Kishimoto H: Effects of TGF- β 1 on the migration and morphology of RAW264.7 cells *in vitro*. *Mol Med Rep* 20: 4331-4339, 2019.
- Wang Z, Gao J, Ohno Y, Liu H and Xu C: Rosiglitazone ameliorates senescence and promotes apoptosis in ovarian cancer induced by Olaparib. *Cancer Chemother Pharmacol* 85: 273-284, 2020.
- Nezu T, Hosomi N, Takahashi T, Anno K, Aoki S, Shimamoto A, Maruyama H, Hayashi T, Matsumoto M and Tahara H: Telomere G-tail length is a promising biomarker related to white matter lesions and endothelial dysfunction in patients with cardiovascular risk: A cross-sectional study. *EBioMedicine* 30: 960-967, 2015.
- Takahashi N, Yamana H, Yoshiki S, Roodman GD, Mundy GR, Jones SJ, Boyde A and Suda T: Osteoclast-like cell formation and its regulation by osteotropic hormones in mouse bone marrow cultures. *Endocrinology* 122: 1373-1382, 1988.
- Guevara I, Iwanekjo J, Dembinska-Kiec A, Pankiewicz J, Wanat A, Anna P, Golabek I, Bartus S, Malczewska-Malec M and Szczudlik A: Determination of nitrite/nitrate in human biological material by the simple Griess reaction. *Clin Chim Acta* 274: 177-188, 1998.
- Kim JH, Lee CH and Lee SW: Exosomal transmission of microRNA from HCV replicating cells stimulates transdifferentiation in hepatic stellate cells. *Mol Ther Nucleic Acids* 14: 483-497, 2019.
- Li Y, Yang Y, Xiong A, Wu X, Xie J, Han S and Zhao S: Comparative gene expression analysis of lymphocytes treated with exosomes derived from ovarian cancer and ovarian cysts. *Front Immunol* 8: 607, 2017.
- Wermuth PJ, Piera-Velazquez S and Jimenez SA: Exosome isolated from serum of systemic sclerosis patients display alterations in their content of profibrotic and antifibrotic microRNA and induce a profibrotic phenotype in cultured normal dermal fibroblasts. *Clin Exp Rheumatol* 35: 21-30, 2017.
- Hashitani S, Urade M, Nishimura N, Maeda T, Takaoka K, Noguchi K and Sakurai K: Apoptosis induction and enhancement of cytotoxicity of anticancer drugs by celecoxib, a selective cyclooxygenase-2 inhibitor, in human head and neck carcinoma cell lines. *Int J Oncol* 23: 665-672, 2003.
- Simonet WS, Lacey DL, Dunstan CR, Kelley M, Chang MS, Luthy R, Nguyen HQ, Wooden S, Bennett L, Boone T, *et al*: Osteoprotegerin: A novel secreted protein involved in the regulation of bone density. *Cell* 89: 309-319, 1997.
- Harding CV, Heuser JE and Stahl PD: Exosomes: Looking back three decades and into the future. *J Cell Biol* 200: 367-371, 2013.
- Raposo G and Stoorvogel W: Extracellular vesicles: Exosomes, microvesicles, and friends. *J Cell Biol* 200: 373-383, 2013.
- Hayflick L and Moorhead PS: The serial cultivation of human diploid cell strains. *Exp Cell Res* 25: 585-621, 1961.
- Campisi J and d'Adda di Fagagna F: Cellular senescence: When bad things happen to good cells. *Nat Rev Mol Cell Biol* 8: 729-740, 2007.
- Zeng X: Human embryonic stem cells: Mechanisms to escape replicative senescence? *Stem Cell Rev* 3: 270-279, 2007.
- Delfarah A, Parrish S, Junge JA, Yang J, Seo F, Li S, Mac J, Wang P, Fraser SE and Graham NA: Inhibition of nucleotide synthesis promotes replicative senescence of human mammary epithelial cells. *J Biol Chem* 294: 10564-10578, 2019.
- Alique M, Bodega G, Giannarelli C, Carracedo J and Ramírez R: MicroRNA-126 regulates hypoxia-inducible factor-1 α which inhibited migration, proliferation, and angiogenesis in replicative endothelial senescence. *Sci Rep* 9: 7381, 2019.
- Gan K, Xu L, Feng X, Zhang Q, Wang F, Zhang M and Tan W: Celastrol attenuates bone erosion in collagen-induced arthritis mice and inhibits osteoclast differentiation and function in RANKL-induced RAW264.7. *Int Immunopharmacol* 24: 239-246, 2015.
- GuezGuez A, Prod'Homme V, Mouska X, Baudot A, Blin-Wakkach C, Rottapel R and Deckert M: 3BP adapter protein is required for receptor activator of NF κ B ligand (RANKL)-induced osteoclast differentiation of RAW264.7. *J Biol Chem* 285: 20952-20963, 2010.
- Itahana K, Campisi J and Dimri GP: Methods to detect biomarkers of cellular senescence: The senescence-associated beta-galactosidase assay. *Methods Mol Biol* 371: 21-31, 2007.
- Dimri GP, Lee X, Basile G, Acosta M, Scott G, Roskelley C, Medrano MM, Linskens M, Rubelj I, Pereira-Smith O, *et al*: A biomarker that identifies senescent human cells in culture and in aging skin *in vivo*. *Proc Natl Acad Sci USA* 92: 9363-9367, 1995.
- Debaq-Chainiaux F, Erusalimsky JD, Campisi J and Toussaint O: Protocols to detect senescence-associated beta-galactosidase (SA- β gal) activity, a biomarker of senescent cells in culture and *in vivo*. *Nat Protoc* 4: 1798-1806, 2009.
- Vogelstein B, Lane DP and Levine AJ: Surfing the p53 network. *Nature* 408: 307-310, 2000.
- Levine AJ and Oren M: The first 30 years of p53: Growing ever more complex. *Nat Rev Cancer* 9: 749-758, 2009.
- Vousden KH and Prives C: Blinded by the light: The Growing complexity of p53. *Cell* 137: 413-431, 2009.
- Feng Z, Zhang H, Levine AJ and Jin S: The coordinate regulation of the p53 and mTOR pathways in cells. *Proc Natl Acad Sci USA* 102: 8204-8209, 2005.
- Budanov AV and Karin M: p53 target genes sestrin1 and sestrin2 connect genotoxic stress and mTOR signalling. *Cell* 134: 451-460, 2008.
- Weichhart T: mTOR as regulator of lifespan, aging, and cellular senescence: A mini-review. *Gerontology* 64: 127-134, 2018.
- Feng Z, Hu W, Teresky AK, Hernandez E, Cordon-Cardo C and Levine AJ: Declining p53 function in the aging process: A possible mechanism for the increased tumor incidence in older populations. *Proc Natl Acad Sci USA* 104: 16633-16638, 2007.
- Campisi J: Aging, cellular senescence, and cancer. *Annu Rev Physiol* 75: 685-705, 2013.
- Soriani A, Zingoni A, Cerboni C, Lannitto ML, Ricciardi RR, Gialleonardo VD, Cipitelli M, Fionda C, Petrucci MT, Guarini A, *et al*: ATM-ATR-dependent up-regulation of DNAM-1 and NKG2D ligands on multiple myeloma cells by therapeutic agents results in enhanced NK-cell susceptibility and is associated with a senescent phenotype. *Blood* 113: 3503-3511, 2009.

45. Coussens LM and Werb Z: Inflammation and cancer. *Nature* 420: 860-867, 2002.
46. Takahashi S, Hakuta M, Aiba K, Ito Y, Horikoshi N, Miura M, Hatake K and Ogata E: Elevation of circulating plasma cytokines in cancer patients with high plasma parathyroid hormone-related protein levels. *Endocr Relat Cancer* 10: 403-407, 2003.
47. Mabrouk N, Ghione S, Laurens V, Plenchette S, Bettaieb A and Paul C: Senescence and cancer: Role of nitric oxide (NO) in SASP. *Cancers (Basel)* 12: 1145, 2020.
48. Campisi J: Senescent cells, tumor suppression, and organismal aging: Good citizens, bad neighbors. *Cell* 120: 513-522, 2015.
49. Farr JN, Kaur J, Doolittle ML and Khosla S: Osteocyte cellular senescence. *Curr Osteoporos Rep* 18: 559-567, 2020.
50. Walsh MC, Kim N, Kadono Y, Rho J, Lee SY, Lorenzo J and Choi Y: Osteoimmunology: Interplay between the immune system and bone metabolism. *Annu Rev Immunol* 24: 33-63, 2006.
51. Azuma Y, Kaji K, Katogi R, Takeshita S and Kudo A: Tumor necrosis factor- α induces differentiation of and bone resorption by osteoclasts. *J Biol Chem* 275: 4858-4864, 2000.
52. Komine M, Kukita A, Kukita T, Ogata Y, Hotokebuchi T and Kohashi O: Tumor necrosis factor- α cooperates with receptor activator of nuclear factor κ B ligand in generation of osteoclasts in stromal cell-depleted rat bone marrow cell culture. *Bone* 28: 474-483, 2001.
53. Palmqvist P, Persson E, Conaway HH and Lerner UH: IL-6, leukemia inhibitory factor, and oncostatin M stimulate bone resorption and regulate the expression of receptor activator of NF- κ B ligand, osteoprotegerin, and receptor activator of NF- κ B in mouse calvariae. *J Immunol* 169: 3353-3362, 2002.
54. Feng W, Liu H, Luo T, Liu D, Du J, Sun J, Wang W, Han X, Yang K, Guo J, *et al*: Combination of IL-6 and sIL-6R differentially regulate varying levels of RANKL-induced osteoclastogenesis through NF- κ B, ERK and JNK signaling pathways. *Sci Rep* 7: 41411, 2017.
55. Yokota K, Sato K, Miyazaki T, Kitaura H, Kayama H, Miyoshi F, Araki Y, Akiyama Y, Takeda K and Mimura T: Combination of tumor necrosis factor α and interleukin-6 induces mouse osteoclast-like cells with bone resorption activity both in vitro and in vivo. *Arthritis Rheumatol* 66: 121-129, 2014.
56. MacIntyre I, Zaidi M, Alam AS, Datta HK, Moonga BS, Lidbury PS, Hecker M and Vane JR: Osteoclastic inhibition: An action of nitric oxide not mediated by cyclic GMP. *Proc Natl Acad Sci USA* 88: 2936-2940, 1991.
57. Kasten TP, Collin-Osdoby P, Patel N, Osdoby P, Krukowski M, Misko TP, Settle SL, Currie MG and Nickols GA: Potentiation of osteoclast bone-resorption activity by inhibition of nitric oxide synthase. *Proc Natl Acad Sci USA* 91: 3569-3573, 1994.
58. Brandi M, Hukkanen M, Umeda T, Moradi-Bidhendi N, Bianchi S, Gross SS, Polak JM and MacIntyre I: Bidirectional regulation of osteoclast function by nitric oxide synthase isoforms. *Proc Natl Acad Sci USA* 92: 2954-2958, 1995.
59. Nathan C and Xie QW: Nitric oxide synthases: Roles, tolls and controls. *Cell* 78: 915-918, 1994.
60. Fukumura D, Kashiwagi S and Jain RK: The role of nitric oxide in tumor progression. *Nat Rev Cancer* 6: 521-534, 2006.
61. Beckman JS, Beckman YW, Chen J, Marshall PA and Freeman BA: Apparent hydroxyl radical production by peroxynitrite: Implications for endothelial injury from nitric and superoxide. *Proc Natl Acad Sci USA* 87: 1620-1624, 1990.
62. Zheng H, Yu X, Collin-Osdoby P and Osdoby P: RANKL stimulates inducible nitric-oxide synthase expression and nitric oxide production in developing osteoclasts. An autocrine negative feedback mechanism triggered by RANKL-induced interferon- β via NF- κ B that restrains osteoclastogenesis and bone resorption. *J Biol Chem* 281: 15809-15820, 2006.
63. Takeda N, O'Dea EL, Doedens A, Kim JW, Weidemann A, Stockmann C, Asagiri M, Simon MC, Hoffmann A and Johnson RS: Differential activation and antagonistic function of HIF-1 α isoforms in macrophages are essential for NO homeostasis. *Genes Dev* 24: 491-501, 2010.
64. Wu C, Rankin EB, Castellini L, Alcludia JF, LaGory EL, Andersen R, Rhodes SD, Wilson TL, Mohammad KS, Castillo AB, *et al*: Oxygen-sensing PHDs regulate bone homeostasis through the modulation of osteoprotegerin. *Genes Dev* 29: 817-831, 2015.
65. Schorey JS, Cheng Y, Singh PP and Smith VL: Exosomes and other extracellular vesicles in host-pathogen interactions. *EMBO Rep* 16: 24-43, 2015.
66. Valadi H, Ekstrom K, Bossios A, Sjostrand M, Lee JJ and Lotvall JO: Exosome-mediated transfer of mRNAs and microRNAs is a novel mechanism of genetic exchange between cells. *Nat Cell Biol* 9: 654-659, 2007.
67. Tkach M and Théry C: Communication by extracellular vesicles: Where we are and where we need to go. *Cell* 164: 1226-1232, 2016.
68. Lehmann BD, Paine MS, Brooks AM, McCubrey JA, Renegar RH, Wang R and Terrian DM: Senescence-associated exosome release from human prostate cancer cells. *Cancer Res* 68: 7864-7871, 2008.
69. Yoshida M, Satoh A, Lin JB, Mills KF, Sasaki Y, Rensing N, Wong M, Apte RS and Imai S: Extracellular Vesicle-contained eNAMPT delays aging and extends lifespan in mice. *Cell Metab* 30: 329-342, 2019.